

## Role of Phe1010 in Light-Induced Structural Changes of the neo1-LOV2 Domain of *Adiantum*<sup>†</sup>

Atsushi Yamamoto,<sup>‡</sup> Tatsuya Iwata,<sup>‡</sup> Satoru Tokutomi,<sup>§</sup> and Hideki Kandori<sup>\*,‡</sup>

Department of Materials Science and Engineering, Nagoya Institute of Technology, Showa-ku, Nagoya 466-8555, Japan, and  
Department of Biological Science, Graduate School of Science, Osaka Prefecture University, 1-1 Gakuencho,  
Sakai, Osaka 599-8531, Japan

Received September 11, 2007; Revised Manuscript Received November 22, 2007

**ABSTRACT:** Phototropin (phot) is a blue-light sensor protein that elicits several photo responses in plants. Phototropin has two flavin mononucleotide (FMN)-binding domains, LOV1 and LOV2, in its N-terminal half. The C-terminal half is a blue-light-regulated Ser/Thr kinase. Various functional studies have reported that only LOV2 is responsible for the kinase activity, whereas the X-ray crystallographic structures of the LOV1 and LOV2 domains are almost identical. How does such a functional difference emerge? Our previous FTIR study of the LOV domains of *Adiantum* neochrome1 (neo1) showed that light-induced protein structural changes are small and temperature independent for neo1-LOV1, whereas the structural changes are large and highly temperature dependent for neo1-LOV2, which involve loops,  $\alpha$ -helices, and  $\beta$ -sheets. These observations successfully explained the different functions in terms of protein structural changes. They also suggested the presence of some crucial amino acids responsible for greater protein structural changes in the LOV2 domain. Here, we focused on phenylalanine-1010 (Phe1010) in neo1-LOV2, where FMN is sandwiched between Phe1010 and the reactive cysteine. Phenylalanine at this position is conserved for LOV2 domains, while the corresponding amino acid is leucine for LOV1 domains in almost all plant phototropins. We observed that unlike wild-type LOV2, the FTIR spectra of F1010L LOV2 exhibited no temperature dependence in the  $\alpha$ -helical and  $\beta$ -sheet regions and that spectral changes in amide-I of these regions were significantly reduced, which was similar to LOV1. Thus, the replacement of phenylalanine with leucine converts neo1-LOV2 into neo1-LOV1 in terms of protein structural changes that must be related to the different functions. We will discuss the roles of phenylalanine and leucine in the LOV2 and LOV1 domains, respectively.

Phototropin (phot) is a blue-light receptor protein in plants that is involved in phototropism (1), chloroplast movement (2), and stomatal opening (3). Higher complex plants have two isoforms of phot, phot1 and phot2, which possess different sensitivities to light (4). *Adiantum* also has a chimerical protein of the chromophore domain of phytochrome and phototropin, which had been called phytochrome3 (5) but recently was renamed neochrome1 (6). Neochrome1 acts as a red- and blue-light sensor for *Adiantum* in its survival in the canopy of forests (7, 8). Phot is composed of ~1000 amino acid residues and two prosthetic FMN<sup>1</sup> molecules. The two FMN-binding domains (ca. 100 residues) are named LOV (light, oxygen, and voltage sensing) domains, which are a subset of the PAS (Per-Arnt-Sim) superfamily. In phot, the LOV1 and LOV2 domains are located at the N-terminal half, and the C-terminal half has a Ser/Thr kinase motif. Thus, the photochemical reaction

of FMN yields kinase activation through the domain–domain interaction, although the mechanism remains unclear. LOV domains have characteristic absorptions at about 450 nm, so that they look yellow. Light absorption of FMN leads to the formation of a triplet excited state that absorbs at about 660 nm. The intersystem crossing takes place with a time constant of 3 ns in *Adiantum* neo1-LOV2 and oat phot1-LOV2 (9). Then, a ground state intermediate is formed that absorbs at 390 nm (S390 intermediate). It is now known that the reaction is an adduct formation between FMN and a nearby cysteine (10–14). Adduct formation takes place with a time constant of 4  $\mu$ s in oat phot2-LOV2 (12) and with a time constant of 0.9 and 4  $\mu$ s in *Chlamydomonas* phot-LOV1 (15). Since S390 is the sole intermediate in the photocycle of LOV domains, it is believed that S390 activates the kinase domain.

An interesting question is why does phot have two LOV domains? Previous molecular biological experiments using expression in insect cells and transgenic *Arabidopsis* reported that only the photochemical reaction of LOV2 is necessary for kinase activation and that phototropin works even if LOV1 does not respond to light for both phot1 and phot2 (16). This result implies that the LOV2 domain is only functionally important in phot. Quantum efficiencies of the photoreaction were about 10 and 2 times higher in the LOV2

<sup>†</sup> This work was supported by grants from the Japanese Ministry of Education, Culture, Sports, Science, and Technology to H.K. (15076202).

<sup>\*</sup> To whom correspondence should be addressed. Phone/fax: 81-52-735-5207; e-mail: kandori@nitech.ac.jp.

<sup>‡</sup> Nagoya Institute of Technology.

<sup>§</sup> Osaka Prefecture University.

<sup>1</sup> Abbreviations: FMN, flavin mononucleotide; LOV, light–oxygen–voltage; PAS, Per-Arnt-Sim; FTIR, Fourier transform infrared; UV, ultraviolet.

|               |     |            | $\beta$ C  | $\beta$ D  | $\beta$ E  |            |      |
|---------------|-----|------------|------------|------------|------------|------------|------|
| Ac_neo1_LOV1  | 729 | REALAQGTGT | FCGRLLNYRK | DGSSFWNLLT | IAPIKDDLGS | IVKLIGVQLE | 778  |
| At_phot1_LOV1 | 251 | RETLAAGN-N | YCGRILNYKK | DGTSFWNLLT | IAPIKDESGK | VLKFIGMQVE | 299  |
| As_phot1_LOV1 | 190 | RQALANGS-N | YCGRVLNYKK | DGTAFWNLLT | IAPIKDEEGR | VLKFIGMQVE | 238  |
| Os_phot1_LOV1 | 190 | RQSLANGS-N | YCGRILNYKK | DGTPFWNLLT | IAPIKDEDGR | LLKFIGMQVE | 238  |
| Zm_phot1_LOV1 | 181 | RQALAAGS-N | YCGRILNYKK | DGTPFWNLLT | VAPIKDEDGR | VLKFIGMQVE | 229  |
| At_phot2_LOV1 | 187 | RDCVKNGK-S | YCGRLLNYKK | DGTPFWNLLT | VTPIKDDQGN | TIKFIGMQVE | 235  |
| Os_phot2_LOV1 | 156 | RDAVKHGR-S | FCGRLLNYRK | DGAPFWNLLT | VTPIRDDNGK | VIKFIGMQVE | 204  |
| Ac_phot_LOV1  | 333 | RECISKGS-G | YCGRLLNYKK | DGSAFWNLLT | ISPIKDVDGS | VLKYIGMQVE | 381  |
| Cr_phot_LOV1  | 74  | RDAIKKE-A  | CSVRLLYNKK | DGTPFWNLLT | VTPIKTPDGR | VSKFVGQVD  | 122  |
| Ac_neo1_LOV2  | 983 | RDAVKEQR-D | VTVQVLNYTK | GGRAFWNLFH | LQVMDENGD  | VQYFIGVQDE | 1031 |
| At_phot1_LOV2 | 529 | RDAIDNQT-E | VTVQLINYTK | SGKKFWNLIF | LQPMRDQKGE | VQYFIGVQLD | 577  |
| As_phot1_LOV2 | 467 | RDAIDNQT-E | VTVQLINYTK | SGKKFWNLIF | LQPMRDQKGD | VQYFIGVQLD | 515  |
| Os_phot1_LOV2 | 467 | RDAIDNQA-E | VTVQLINYTK | SGKKFWNLIF | LQPMRDQKGD | VQYFIGVQLD | 515  |
| Zm_phot1_LOV2 | 455 | RDAIDNQT-E | VTVQLINYTK | SGKKFWNLIF | LQPMRDQKGD | VQYFIGVQLD | 503  |
| At_phot2_LOV2 | 443 | RDAIRDQR-E | ITVQLINYTK | SGKKFWNLIF | LQPMRDQKGE | LQYFIGVQLD | 491  |
| Os_phot2_LOV2 | 442 | REAIREQK-E | ITVQLINYTK | SGKKFWNLIF | LQPMRDQKGE | LQYFIGVQLD | 490  |
| Ac_phot_LOV2  | 621 | RDAIDNEK-E | VTVQLLYNKK | TGRTFWNLIF | LQPMRDHKGE | LQYFTGVQLD | 669  |
| Cr_phot_LOV2  | 267 | RAAIKEGS-E | LTVRILNYTK | AGKAFWNMFT | LAPMRDQDGH | ARFFVGQVD  | 315  |

FIGURE 1: Sequence alignment of phototropin LOV domains.  $\beta$ -Sheet structure is noted as arrows above the alignment. Residues in gray form (left side) conserved different amino acids among LOV1 and LOV2, whereas residues in gray form (right side) conserved glutamine in both LOV1 and LOV2.

domain than in the LOV1 domain for *Arabidopsis* phot1 and phot2, respectively (10, 17). Higher quantum efficiency of LOV2 is consistent with its functional importance. Size exclusion chromatography (18) and small-angle X-ray scattering (SAXS) analysis (19) of LOV1 suggest that this domain may play a role in receptor dimerization. A recent in vitro study found that LOV2 prohibits constitutively active kinase by binding to the kinase domain directly (20). The LOV2 domain, thus, acts as a light-regulated molecular switch of the phot kinase. In contrast, LOV1 was found to act as an attenuator for the light sensitivity of the switch (20). In spite of these functional differences between LOV1 and LOV2, X-ray crystallographic structures of the LOV1 domain of *Chlamydomonas* phot (21) and the LOV2 domain of *Adiantum* neo1 (22) were surprisingly similar. This suggests that the detailed structures and/or structural changes are different between LOV1 and LOV2 domains. How is such a functional difference created from a similar protein architecture? Recent MD simulations suggested a different structural flexibility between LOV1 and LOV2 (23). Our FTIR spectroscopic studies reported highly different protein structural changes between the LOV1 and the LOV2 domains of *Adiantum* neochrome1 (neo1; previously called phytochrome3, phy3). In the case of neo1-LOV2, progressive protein structural changes were observed involving  $\alpha$ -helix and  $\beta$ -sheet regions (24), suggesting the presence of global protein structural changes. In contrast, protein structural changes were very small in neo1-LOV1, which was almost temperature independent (25). Therefore, we interpret that LOV1 does not work for light sensing and concluded that plants utilize a unique protein architecture (LOV domain) for different functions by regulating their protein structural changes. While these spectroscopic results explain well different functions of LOV1 and LOV2, two questions remain: What determines such a difference in protein structural changes? Are there any specific amino acids responsible for such a functional difference? Figure 1 shows the amino acids of each family of LOV1 and LOV2 in the region of the  $\beta$ -sheet of the LOV core because the  $\beta$ -sheet structure is altered only in neo1-LOV2 during the photocycle (25). In the present study, we focused on phenylalanine-1010 (Phe1010) in neo1-LOV2. Phe1010 and the reactive cysteine

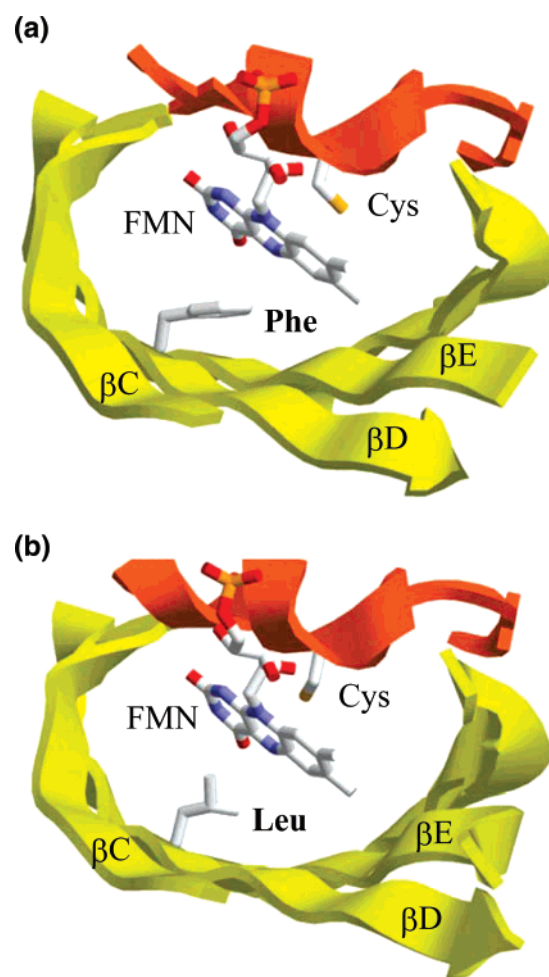


FIGURE 2: X-ray crystallographic structures of (a) *Adiantum* neo1-LOV2 (PDB ID 1G28) and (b) *Chlamydomonas* phot-LOV1 (PDB ID 1N9N) in the dark states. FMN is indicated by a stick drawing, and C, N, and O atoms are white, blue, and red, respectively. Reactive cysteine and leucine or phenylalanine also are indicated by a stick drawing.  $\beta$ -Sheet structures are in yellow ribbons, and  $\beta$ C,  $\beta$ D, and  $\beta$ E that form a major backbone of the  $\beta$ -scaffold are labeled.

sandwich FMN (Figure 2a). Phenylalanine at this position is conserved for LOV2, while the corresponding amino acid

for LOV1 is leucine in almost all plant phototropins (Figure 2b). We measured the UV-vis and FTIR spectra of the F1010L mutant of neo1-LOV2 under the same conditions for neo1-LOV2 and neo1-LOV1. Unlike in the wild-type LOV2, the FTIR spectra of F1010L exhibited no temperature dependence in the  $\alpha$ -helical and  $\beta$ -sheet regions, and spectral changes in amide-I were significantly reduced, which was similar to LOV1. Thus, the replacement of phenylalanine with leucine converted LOV2 into LOV1 in terms of protein structural changes, although the conversion was not complete. The photocycle of F1010L neo1-LOV2 was much longer than that of wild-type neo1-LOV2, and the photocycle kinetics property shifted from the LOV2-type to the LOV1-type. We thus concluded that Phe1010 is one of the determinants of the characteristics of the LOV2 domain.

## MATERIALS AND METHODS

**Sample Preparation.** The construct containing N-terminal CBP and spanning amino acid residues 905–1087 of neo1, which include the J $\alpha$  helix (26), was expressed in *Escherichia coli* BL21 (DE3) pLysS cells (Novagen). Overexpression and purification of the CBP-neo1-LOV2F1010L mutant were carried out by the same procedure as those of CBPneo1-LOV2 (24). The neo1-LOV2F1010L mutant gene was constructed by PCR using a QuikChange site-directed mutagenesis kit (Stratagene). The oligonucleotide primers were 5'-GCCTTCTGGAACCTCCTGCACCTGCAGGT-CATGCGGGAC-3' and 5'-GTCCCGCATGACCTGCAG-GTGCAGGAGGTTCCAGAAGGC-3'. The desired mutation was confirmed by DNA sequencing. The purified protein was concentrated to give a final concentration of 2.5 mg/mL by using a Microcon YM-10 instrument (Millipore) and dialyzed against 1 mM K/phosphate buffer (pH 7). A total of 70–80  $\mu$ L of the solution was placed on a BaF2 window, and the dry films were hydrated by dropping H<sub>2</sub>O next to the film on the window. Hydration conditions for the neo1-LOV2F1010L mutant and neo1-LOV2 were identical.

**Spectroscopy.** UV-vis and infrared spectra of the hydrated films were measured using V-550DS (JASCO) and FTS-40 (Bio-Rad) spectrophotometers, respectively, as described previously (24, 25, 27). Low-temperature spectra were measured by using a cryostat (Optistat DN) and a temperature controller (ITC 4) with liquid nitrogen as the coolant. Hydrated films were illuminated by >400 nm light, which was supplied with a combination of a halogen-tungsten lamp (1000 W) and a long-pass filter (L42, Asahi Techno Glass). Photocycle kinetics experiments were performed for the protein solution of the neo1-LOV2F1010L mutant in 50 mM K/phosphate (pH 7). A dark reversion process from S390 to the original state was monitored at 475 nm by using a UV-2400PC (Shimadzu).

## RESULTS

**UV-vis Spectra of the F1010L Mutant and Wild-Type Proteins.** Figure 3 shows light minus dark difference UV-vis spectra of the wild-type (dashed line) and F1010L mutant (solid line) proteins of neo1-LOV2 measured at 295 K. The spectrum of the wild-type is identical to those reported previously (24). The spectrum of F1010L is very similar to that of the wild-type, indicating that S390 is formed in the F1010L mutant. Almost identical difference spectra were

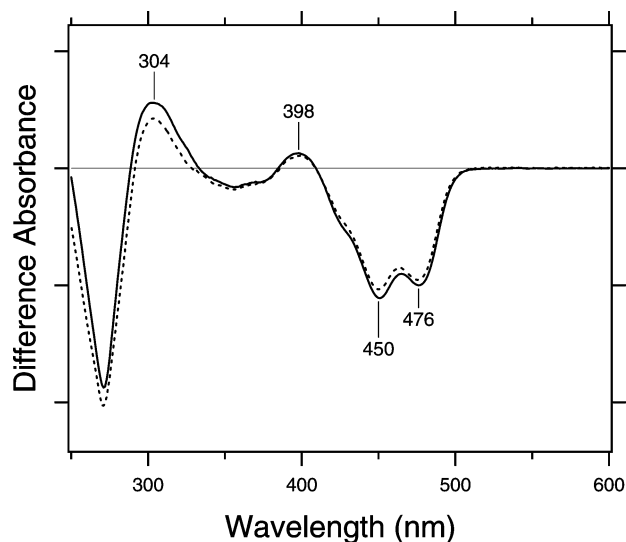


FIGURE 3: Light minus dark difference spectra for the wild-type (dashed line) and F1010L mutant (solid line) proteins of neo1-LOV2 in the UV-vis region. The spectra were recorded at 295 K. One division of the y-axis corresponds to 0.05 absorbance units.

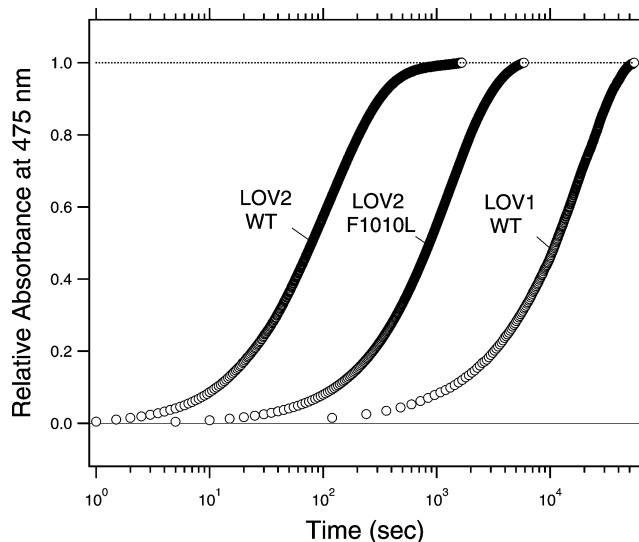


FIGURE 4: Time course of the dark recoveries of neo1-LOV1, the wild-type neo1-LOV2, and the F1010L mutant neo1-LOV2 measured at room temperature. Absorptions at 475 nm in the unphotolyzed state are normalized as 1.

obtained for F1010L at lower temperatures (data not shown), indicating that only one photointermediate in the electronically ground state, S390, is formed in the wide temperature range from liquid nitrogen to ambient conditions. Although S390 can be formed at all of the temperatures measured for F1010L, only a part of the unphotolyzed state was photoconverted to S390 at low temperatures, being similar to the wild-type (24). Two negative peaks at 450 and 476 nm and two positive peaks at 304 and 398 nm in the wild-type are preserved in F1010L (Figure 3). Thus, mutation of Phe1010 to Leu does not change the absorption spectra of the unphotolyzed and S390 states of neo1-LOV2. This may be reasonable because absorption spectra are almost identical between neo1-LOV1 and neo1-LOV2 (25).

**Thermal Reversion of S390 to the Original State.** Figure 4 shows the dark reversion processes from the S390 intermediate to the original state by monitoring the absorption at 475 nm. They were measured for the LOV domains in



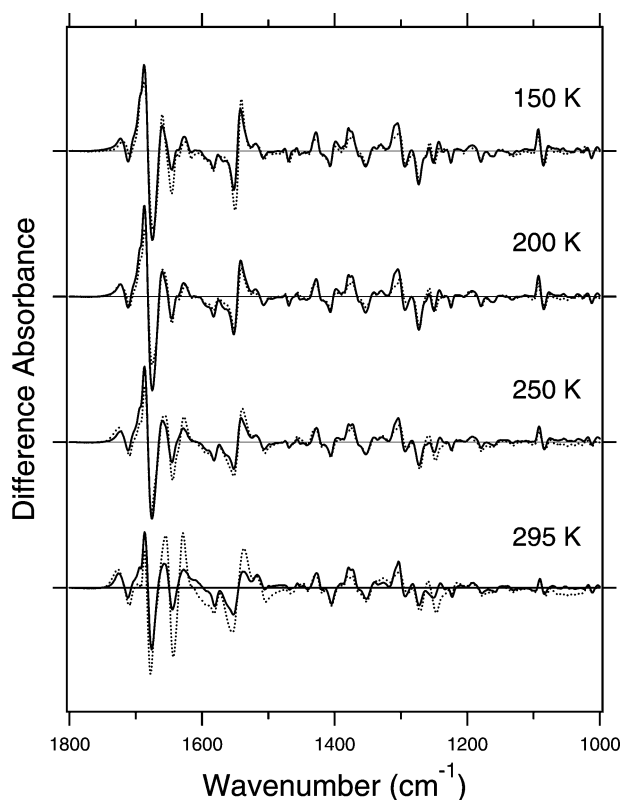


FIGURE 5: Light minus dark infrared spectra for neo1-LOV2 wild-type (dotted line) and F1010L mutant (solid line) in the 1800–1000  $\text{cm}^{-1}$  region. Spectra were measured at 150, 200, 250, and 295 K. One division of the y-axis corresponds to 0.006 absorbance units.

solution at 295 K. Kinetics were compared among neo1-LOV1, neo1-LOV2, and the F1010L mutant protein of neo1-LOV2. The half-lifetimes ( $t_{1/2}$ ) were 90 s for neo1-LOV2 and 3.1 h for neo1-LOV1, while the lifetime of S390 in the F1010L mutant protein of neo1-LOV2 was 870 s. The lifetimes of S390 in LOV2 became 10 times longer, presumably because of the mutation at position 1010. The photocycle kinetics property of F1010L seems to be shifted from the neo1-LOV2-type to the neo1-LOV1-type, although it is still shorter than that of neo1-LOV1 (Figure 4).

We previously reported that the photocycle kinetics of the Q1029L mutant of neo1-LOV2 became 7.2 times longer (25), indicating that Gln1029 is an important residue for neo1-LOV2. It is, however, noted that Gln1029 is conserved in both LOV1 and LOV2, and hence, the amino acid does not characterize LOV1 and LOV2. In contrast, the amino acid residue at position 1010 is Phe and Leu in neo1-LOV2 and -LOV1, respectively, which are highly conserved in many plants (Figure 1). Thus, this amino acid is suggested to be crucial for characterizing the LOV1 and LOV2 domains in neochrome1. To further confirm this idea, we tried to prepare the L757F mutant of neo1-LOV1. However, the mutant protein did not bind FMN.

**Low-Temperature FTIR Spectra of the F1010L Mutant and Wild-Type Proteins.** Figure 5 compares light minus dark difference FTIR spectra of the wild-type (dotted line) and F1010L mutant (solid line) neo1-LOV2 in the 1800–1000  $\text{cm}^{-1}$  region, where the same hydrated films were used for the UV-vis (Figure 3) and FTIR (Figure 5) measurements. We observed a negative S–H stretch at 2566  $\text{cm}^{-1}$  for the wild-type and F1010L mutant neo1-LOV2 at all temperatures

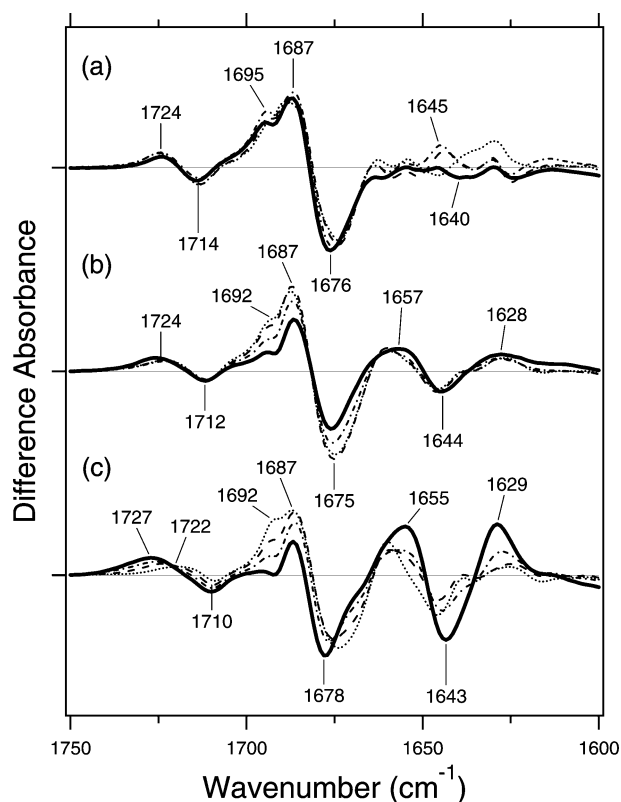


FIGURE 6: Light minus dark infrared spectra for neo1-LOV1 wild-type (a), neo1-LOV2 F1010L mutant (b), and neo1-LOV2 wild-type (c) proteins in the 1750–1600  $\text{cm}^{-1}$  region. Spectra were measured at 150 K (dotted lines), 200 K (dashed-dotted lines), and 295 K (solid lines). One division of the y-axis corresponds to 0.009 absorbance units.

(data not shown), which is consistent with the fact that the F1010L mutant forms a flavin-cysteinyl adduct similar to the wild-type. Here, each FTIR spectrum was normalized by the negative band at 2566  $\text{cm}^{-1}$ . In the 1500–1000  $\text{cm}^{-1}$  region of Figure 5, both spectra are almost superimposable at all temperatures measured from 150 to 295 K, except for the small spectral deviation at 1270–1230  $\text{cm}^{-1}$ . Previous  $^{13}\text{C}$ -isotope labeling of the chromophore and protein showed that these spectra contain both chromophore and protein vibrations (28).

In contrast to the 1500–1000  $\text{cm}^{-1}$  region, a highly different spectral feature was obtained in the 1750–1600  $\text{cm}^{-1}$  region, which represents characteristic frequencies of amide-I vibrations, and C=O stretches of the peptide backbone. The C=O stretching vibrations of the FMN chromophore also appear at 1686(+)/1677(–) and 1730(+)/1711(–)  $\text{cm}^{-1}$  (C(2)=O and C(4)=O stretches, respectively). Figure 6 shows the difference FTIR spectra of neo1-LOV1 (Figure 6a), F1010L neo1-LOV2 (Figure 6b), and neo1-LOV2 (Figure 6c) in the 1750–1600  $\text{cm}^{-1}$  region measured at 150, 200, 250, and 295 K.

The spectrum of F1010L at 150 K (Figure 6b, dotted line) has peaks at 1724 (+), 1712 (–), 1692 (+), 1687 (+), 1675 (–), 1657 (+), 1644 (–), and 1628 (+)  $\text{cm}^{-1}$ . The peak pair at 1724(+)/1712 (–)  $\text{cm}^{-1}$  originates from the C(4)=O stretch of FMN (28). The corresponding negative peak of the wild-type is at 1710  $\text{cm}^{-1}$ , indicating that the hydrogen bond of the C(4)=O group is slightly weaker in F1010L than in the wild-type. The bands at 1692 (+) and 1687 (+)  $\text{cm}^{-1}$  are attributed to the amide-I vibrations of the loop structures

and the C(2)=O stretch of FMN, respectively, while the band at 1675 (–)  $\text{cm}^{-1}$  also originates from the amide-I vibrations of the loop structures and C(2)=O stretch of FMN (28). The bands at 1657 (+) and 1628 (+)  $\text{cm}^{-1}$  are attributed to the amide-I vibrations of the  $\alpha$ -helix and  $\beta$ -sheet structures, respectively, while that at 1644 (–)  $\text{cm}^{-1}$  also originates from the amide-I vibrations of the  $\alpha$ -helix and  $\beta$ -sheet structures. These spectral features of F1010L at 150 K are similar to that of the wild-type neo1-LOV2 (Figure 6c, dotted line).

Although the spectral features at 150 K (Figure 6, dotted lines) are similar between F1010L (Figure 6b) and wild-type (Figure 6c) neo1-LOV2, their temperature dependences were considerably different. Figure 6b shows a temperature-dependent spectral alteration at 1700–1660  $\text{cm}^{-1}$  but almost no temperature dependence at 1660–1600  $\text{cm}^{-1}$ . This is entirely different from that of the wild-type neo1-LOV2 (Figure 6c), where the obtained FTIR spectra are highly temperature dependent at all frequencies. In the case of the wild-type neo1-LOV2, the positive 1692  $\text{cm}^{-1}$  band at 150 K disappears at 295 K (Figure 6c) because the amide-I band of the loop region shows a low-frequency shift from 1678  $\text{cm}^{-1}$  (28). On the other hand, two peaks are intensified at 1655 and 1629  $\text{cm}^{-1}$  in the spectrum at 295 K (Figure 6c), the latter of which was identified as the amide-I vibration of the  $\beta$ -sheet region (28). We thus defined the S390 states at 150 and 295 K as S390I and S390II, respectively, whose protein structural changes are different (29, 30). In F1010L, the 1692  $\text{cm}^{-1}$  band is reduced at higher temperatures but still observed even at 295 K, unlike the wild-type (Figure 6b). F1010L exhibits a positive band at 1628  $\text{cm}^{-1}$ , but it shows no temperature dependence (Figure 6b). These results clearly show that temperature-dependent secondary structural alterations in S390 are limited in F1010L. The protein structure of F1010L at 295 K is more like S390I than S390II. Nevertheless, it is not the S390I state because relaxation of the loop region takes place as is shown by the decrease of the 1692  $\text{cm}^{-1}$  band (Figure 6b).

The spectral feature and temperature dependence in the  $\alpha$ -helical and  $\beta$ -sheet regions of F1010L (Figure 6b) resemble those of neo1-LOV1 (Figure 6a) rather than those of neo1-LOV2 (Figure 6c). Figure 6a shows that neo1-LOV1 lacks temperature-dependent protein structural changes. Characteristic temperature dependence was not only seen for the amide-I bands but also for the C(4)=O stretch of FMN at 1730–1700  $\text{cm}^{-1}$ . Temperature dependence of this band in neo1-LOV2 (Figure 6c) diminishes in neo1-LOV1 (Figure 6a) and F1010L neo1-LOV2 (Figure 6b). Thus, we conclude that temperature-dependent protein structural changes characteristic of neo1-LOV2 are significantly reduced by the mutation at position 1010. In the wild-type neo1-LOV2, the S390I to S390II transition accompanies (i) structural relaxation of the loop region and (ii) structural perturbation of the  $\beta$ -sheet region. In the case of F1010L, it is likely that relaxation of the loop region partially takes place, without structurally perturbing the  $\beta$ -sheet region. The unchanged  $\beta$ -sheet region in F1010L may be correlated with the temperature-independent C(4)=O stretching vibrations in S390 because the C(4)=O group forms a hydrogen bond with Asn1008 that is located on the same  $\beta$ -strand with Phe1010.

## DISCUSSION

Structural similarity and functional difference between the LOV1 and the LOV2 domains have been one of the important issues in the study of phototropin. The recent MD simulations suggested that the LOV1 activation is likely caused by a change in hydrogen bonding between protein and ligand that destabilizes a highly conserved salt bridge, whereas the LOV2 activation seems to result from a change in the flexibility of a set of protein loops (23). We previously reported highly different protein structural changes between the LOV1 and the LOV2 domains of the *Adiantum* neochrome1 (25). While these spectroscopic results could explain well the different functions of LOV1 and LOV2, the question as to what determines such differences in protein structural changes still remains. In this paper, we discuss the role of Phe1010, which is highly conserved in LOV2 domains. Phe1010 is localized between FMN and  $\beta$ -sheet of the LOV core, and the corresponding amino acid is leucine in the LOV1 domains (Figure 2).

Like the wild-type, only S390 was observed as a stable intermediate for F1010L. UV–vis absorption spectra of the unphotolyzed and S390 states are identical between wild-type and F1010L (Figure 3). Formation of S390 was reduced at low temperatures for both the wild-type and the F1010L mutant. These results demonstrate that the mutation at the F1010 position hardly influences the local structure around the FMN chromophore in the neo1-LOV2 domain. In spite of these similarities, we observed a clear difference in protein structural changes and photocycle kinetics between F1010L and wild-type neo1-LOV2.

The C(4)=O stretch of FMN was almost temperature independent for F1010L (Figure 6b). In the case of wild-type, the C(4)=O stretch of FMN is temperature independent for the unphotolyzed state (1710  $\text{cm}^{-1}$ ) but highly temperature dependent for the S390 intermediate (Figure 6c). The C(4)=O stretch in S390 shifts from 1722  $\text{cm}^{-1}$  at 150 K to 1727  $\text{cm}^{-1}$  at 295 K (Figure 6c). This change is presumably correlated with the temperature-dependent structural changes of the  $\beta$ -sheet region for the wild-type. Such temperature dependence of the C(4)=O stretch in neo1-LOV2 also diminishes in neo1-LOV1 (25) and the Q1029L mutant of neo1-LOV2 (27), where protein structural changes are much smaller than in neo1-LOV2. The C(4)=O group forms a hydrogen bond with Asn1008, which is located on the  $\beta$ D-strand of the LOV core (Figure 7). Therefore, the temperature dependence of the C(4)=O stretch of FMN (positive bands at 1730–1720  $\text{cm}^{-1}$ ) and the amide-I band of the  $\beta$ -sheet (positive band at about 1630  $\text{cm}^{-1}$ ) is likely to be correlated. The present study clearly shows that F1010L lacks temperature dependence in the frequency regions associated with FMN C(4)=O and  $\beta$ -sheet (Figure 6b), suggesting that Phe1010 plays an important role in intramolecular signal transduction (Figure 7).

Protein structures of S390I and S390II are now better established. In wild-type neo1-LOV2, a single intermediate state (S390) can be classified into two conformations. S390I is the early photointermediate that alters the loop region presumably nearby the reactive cysteine, while the other ( $\beta$ -sheet) side is unchanged (Figure 2). S390II is the late and probably active photointermediate that alters the loop region differently from S390I, where the  $\beta$ -sheet region of the LOV

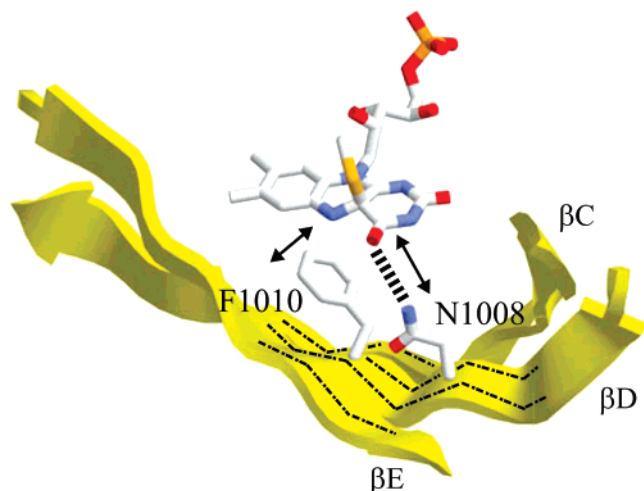


FIGURE 7: Protein structural changes upon formation of S390 are schematically drawn on the structure of *Adiantum* neo1-LOV2 (PDB ID 1JNU). The adduct formation between FMN and cysteine may cause a conformational change at phenylalanine, which is the driving force for the structural change at the  $\beta$ -sheet region in neo1-LOV2 (yellow ribbons).

core is structurally perturbed. From the FTIR results (25), S390I is formed, but not S390II, in neo1-LOV1. Two amino acids, Gln1029 and Phe1010, are important for the transition from S390I to S390II because S390II is not produced in the Q1029L (27) and F1010L (present study) mutants of neo1-LOV2. However, we infer that the roles of Gln1029 and Phe1010 are different because Gln1029 is conserved in both LOV1 and LOV2, while Phe1010 is unique to LOV2. Previous X-ray crystallography of the unphotolyzed (22) and S390 (14) states of neo1-LOV2 showed switching of a hydrogen bond between Gln1029 and FMN, which is also common for the LOV1 domains (21). Thus, the important role of Gln1029 is presumably common between LOV1 and LOV2. In contrast, it is likely that Phe1010 is an amino acid that characterizes LOV2.

Then, what is the mechanism to drive the S390I to S390II transition assisted by Phe1010? The  $\pi$ - $\pi$  interaction between FMN and Phe1010 is a possible candidate, although we did not observe any spectral changes in UV-vis absorption (Figure 3). The distances of the nearest atom between FMN and Phe1010 are 3.20 Å (N(5) atom of FMN and C(E1) atom of Phe) and 3.58 Å (C(5a) atom of FMN and C(Z) atom of Phe) for the unphotolyzed and S390 states, respectively, according to the X-ray structures (14, 22). This suggests that the adduct formation induces orientational changes of the side chain of Phe1010, which may be correlated with the structural perturbation of the  $\beta$ -sheet (Figure 7). It should, however, be noted that further experimental and theoretical efforts are requested for a better understanding. In particular, the role of Phe1010 in protein dynamics should be investigated in more detail.

The recovery from S390 to the original state was 10 times slower in F1010L. The slow photocycle kinetics is characteristic of neo1-LOV1 but not of neo1-LOV2 (Figure 4). The Q1029L mutant also shows slow kinetics (25). Our data suggest that the photocycle kinetics is slowed if S390I is trapped. In other words, the S390I state possesses a longer lifetime than S390II. This sounds interesting but somewhat controversial because S390II accompanies greater protein structural changes. Alexandre et al. recently reported the

base-catalyzed mechanism for the cleavage of the adduct between FMN and reactive cysteine (31). Therefore, we suggest that large structural perturbation in S390II gives a higher probability of the adduct cleavage than S390I, although the catalyst is unclear in this case. Recently, Christie et al. identified a highly conserved isoleucine residue within the LOV2 domain that plays an important role in the stabilization of LOV390 that is formed upon photoexcitation, and the steric role of this isoleucine is independent of the reported base-catalyzed mechanism (32). Thus, several factors are likely to contribute to the mechanism of adduct decay.

Harper et al. reported the presence of an additional  $\alpha$ -helix (the  $J\alpha$ -helix) by means of NMR spectroscopy (26). The  $J\alpha$ -helix only exists in the C-terminus of the LOV2 domains of phototropin in many plants, and it was found that the interaction between the LOV core and the  $J\alpha$ -helix is important for autophosphorylation of phototropin (33). The importance of the  $J\alpha$ -helix has also been emphasized by other spectroscopic techniques (34–36). Together with the present observation, the light-signaling pathway in LOV2 is likely to be (i) an adduct formation between FMN and Cys966 that accompanies structural perturbation of the loop region (S390I), (ii) a structural perturbation of the  $\beta$ -sheet that involves Phe1010 and Gln1029 (S390II), and (iii) release of the  $J\alpha$ -helix from the  $\beta$ -sheet of the LOV core.

## REFERENCES

1. Liscum, E., and Briggs, W. R. (1995) Mutations in the NPH1 locus of *Arabidopsis* disrupt the perception of phototropic stimuli, *Plant Cell* 7, 473–485.
2. Kagawa, T., Sakai, T., Suetsugu, N., Oikawa, K., Ishiguro, S., Kato, T., Tabata, S., Okada, K., and Wada, M. (2001) *Arabidopsis* NPL1: A phototropin homologue controlling the chloroplast high-light avoidance response, *Science* 291, 2138–2141.
3. Kinoshita, T., Doi, M., Suetsugu, N., Kagawa, T., Wada, M., and Shimazaki, K. (2001) Phot1 and phot2 mediate blue light regulation of stomatal opening, *Nature* 414, 656–660.
4. Sakai, T., Kagawa, T., Kasahara, M., Swartz, T. E., Christie, J. M., Briggs, W. R., Wada, M., and Okada, K. (2001) *Arabidopsis* nph1 and npl1: Blue light receptors that mediate both phototropism and chloroplast relocation, *Proc. Natl. Acad. Sci. U.S.A.* 98, 6969–6974.
5. Christie, J. M., Salomon, M., Nozue, K., Wada, M., and Briggs, W. R. (1999) LOV (light, oxygen, or voltage) domains of the blue-light photoreceptor phototropin (nph1): Binding sites for the chromophore flavin mononucleotide, *Proc. Natl. Acad. Sci. U.S.A.* 96, 8779–8783.
6. Suetsugu, N., Mittmann, F., Wagner, G., Hughes, J., and Wada, M. (2005) A chimeric photoreceptor gene, NEOCHROME, has arisen twice during plant evolution, *Proc. Natl. Acad. Sci. U.S.A.* 102, 13705–13709.
7. Kawai, H., Kanegae, T., Christensen, S., Kiyosue, T., Sato, Y., Imaizumi, T., Kadota, A., and Wada, M. (2003) Responses of ferns to red light are mediated by an unconventional photoreceptor, *Nature* 421, 287–290.
8. Kanegae, T., Hayashida, E., Kuramoto, C., and Wada, M. (2006) A single chromoprotein with triple chromophores acts as both a phytochrome and a phototropin, *Proc. Natl. Acad. Sci. U.S.A.* 103, 17997–18001.
9. Kennis, J. T., Crosson, S., Gauden, M., van Stokkum, I. H., Moffat, K., and van Grondelle, R. (2003) Primary reactions of the LOV2 domain of phototropin, a plant blue-light photoreceptor, *Biochemistry* 42, 3385–3392.
10. Salomon, M., Christie, J. M., Knieb, E., Lempert, U., and Briggs, W. R. (2000) Photochemical and mutational analysis of the FMN-binding domains of the plant blue light receptor, phototropin, *Biochemistry* 39, 9401–9410.



11. Miller, S. M., Massey, V., Ballou, D., Williams, C. H., Jr., Distefano, M. D., Moore, M. J., and Walsh, C. T. (1990) Use of a site-directed triple mutant to trap intermediates: Demonstration that the flavin C(4a)-thiol adduct and reduced flavin are kinetically competent intermediates in mercuric ion reductase, *Biochemistry* 29, 2831–2841.
12. Swartz, T. E., Corchnoy, S. B., Christie, J. M., Lewis, J. W., Szundi, I., Briggs, W. R., and Bogomolni, R. A. (2001) The photocycle of a flavin-binding domain of the blue light photoreceptor phototropin, *J. Biol. Chem.* 276, 36493–36500.
13. Salomon, M., Eisenreich, W., Durr, H., Schleicher, E., Knieb, E., Massey, V., Rudiger, W., Muller, F., Bacher, A., and Richter, G. (2001) An optomechanical transducer in the blue light receptor phototropin from *Avena sativa*, *Proc. Natl. Acad. Sci. U.S.A.* 98, 12357–12361.
14. Crosson, S., and Moffat, K. (2002) Photoexcited structure of a plant photoreceptor domain reveals a light-driven molecular switch, *Plant Cell* 14, 1067–1075.
15. Kottke, T., Heberle, J., Hehn, D., Dick, B., and Hegemann, P. (2003) Phot-LOV1: Photocycle of a blue-light receptor domain from the green alga *Chlamydomonas reinhardtii*, *Biophys. J.* 84, 1192–1201.
16. Christie, J. M., Swartz, T. E., Bogomolni, R. A., and Briggs, W. R. (2002) Phototropin LOV domains exhibit distinct roles in regulating photoreceptor function, *Plant J.* 32, 205–219.
17. Kasahara, M., Swartz, T. E., Olney, M. A., Onodera, A., Mochizuki, N., Fukuzawa, H., Asamizu, E., Tabata, S., Kanegae, H., Takano, M., Christie, J. M., Nagatani, A., and Briggs, W. R. (2002) Photochemical properties of the flavin mononucleotide-binding domains of the phototropins from *Arabidopsis*, rice, and *Chlamydomonas reinhardtii*, *Plant Physiol.* 129, 762–773.
18. Salomon, M., Lempert, U., and Rudiger, W. (2004) Dimerization of the plant photoreceptor phototropin is probably mediated by the LOV1 domain, *FEBS Lett.* 572, 8–10.
19. Nakasako, M., Iwata, T., Matsuoka, D., and Tokutomi, S. (2004) Light-induced structural changes of LOV domain-containing polypeptides from *Arabidopsis* phototropin 1 and 2 studied by small-angle X-ray scattering, *Biochemistry* 43, 14881–14890.
20. Matsuoka, D., and Tokutomi, S. (2005) Blue light-regulated molecular switch of Ser/Thr kinase in phototropin, *Proc. Natl. Acad. Sci. U.S.A.* 102, 13337–13342.
21. Fedorov, R., Schlichting, I., Hartmann, E., Domratheva, T., Fuhrmann, M., and Hegemann, P. (2003) Crystal structures and molecular mechanism of a light-induced signaling switch: The Phot-LOV1 domain from *Chlamydomonas reinhardtii*, *Biophys. J.* 84, 2474–2482.
22. Crosson, S., and Moffat, K. (2001) Structure of a flavin-binding plant photoreceptor domain: Insights into light-mediated signal transduction, *Proc. Natl. Acad. Sci. U.S.A.* 98, 2995–3000.
23. Freddolino, P. L., Dittrich, M., and Schulten, K. (2006) Dynamic switching mechanisms in LOV1 and LOV2 domains of plant phototropins, *Biophys. J.* 91, 3630–3639.
24. Iwata, T., Nozaki, D., Tokutomi, S., Kagawa, T., Wada, M., and Kandori, H. (2003) Light-induced structural changes in the LOV2 domain of *Adiantum* phytochrome3 studied by low-temperature FTIR and UV-visible spectroscopy, *Biochemistry* 42, 8183–8191.
25. Iwata, T., Nozaki, D., Tokutomi, S., and Kandori, H. (2005) Comparative investigation of the LOV1 and LOV2 domains in *Adiantum* phytochrome3, *Biochemistry* 44, 7427–7434.
26. Harper, S. M., Neil, L. C., and Gardner, K. H. (2003) Structural basis of a phototropin light switch, *Science* 301, 1541–1544.
27. Nozaki, D., Iwata, T., Ishikawa, T., Todo, T., Tokutomi, S., and Kandori, H. (2004) Role of Gln1029 in the photoactivation processes of the LOV2 domain in *Adiantum* phytochrome3, *Biochemistry* 43, 8373–8379.
28. Iwata, T., Nozaki, D., Sato, Y., Sato, K., Nishina, Y., Shiga, K., Tokutomi, S., and Kandori, H. (2006) Identification of the C=O stretching vibrations of FMN and peptide backbone by <sup>13</sup>C-labeling of the LOV2 domain of *Adiantum* phytochrome3, *Biochemistry* 45, 15384–15391.
29. Iwata, T., Yamamoto, A., Tokutomi, S., and Kandori, H. (2007) Hydration and temperature similarly affect light-induced protein structural changes in the chromophoric domain of phototropin, *Biochemistry* 46, 7016–7021.
30. Matsuoka, D., Iwata, T., Zikihara, K., Kandori, H., and Tokutomi, S. (2007) Primary processes during the light-signal transduction of phototropin, *Photochem. Photobiol.* 83, 122–130.
31. Alexandre, M. T., Arents, J. C., van Grondelle, R., Hellingwerf, K. J., and Kennis, J. T. (2007) A base-catalyzed mechanism for dark state recovery in the *Avena sativa* phototropin-1 LOV2 domain, *Biochemistry* 46, 3129–3137.
32. Christie, J. M., Corchnoy, S. B., Swartz, T. E., Hokenson, M., Han, I. S., Briggs, W. R., and Bogomolni, R. A. (2007) Steric interactions stabilize the signaling state of the LOV2 domain of phototropin 1, *Biochemistry* 46, 9310–9319.
33. Harper, S. M., Christie, J. M., and Gardner, K. H. (2004) Disruption of the LOV-J $\alpha$  helix interaction activates phototropin kinase activity, *Biochemistry* 43, 16184–16192.
34. Eitoku, T., Nakasone, Y., Matsuoka, D., Tokutomi, S., and Terazima, M. (2005) Conformational dynamics of phototropin 2 LOV2 domain with the linker upon photoexcitation, *J. Am. Chem. Soc.* 127, 13238–13244.
35. Nakasone, Y., Eitoku, T., Matsuoka, D., Tokutomi, S., and Terazima, M. (2007) Dynamics of conformational changes of *Arabidopsis* phototropin 1 LOV2 with the linker domain, *J. Mol. Biol.* 367, 432–442.
36. Chen, E., Swartz, T. E., Bogomolni, R. A., and Kliger, D. S. (2007) A LOV story: The signaling state of the phot1 LOV2 photocycle involves chromophore-triggered protein structure relaxation, as probed by far-UV time-resolved optical rotatory dispersion spectroscopy, *Biochemistry* 46, 4619–4624.

BI701851V